

# Heisenberg scaling of quantum logic spectroscopy with ions in thermal motion

D. Kienzler<sup>\*†1,2</sup>, Y. Wan<sup>\*1,2</sup>, S. D. Erickson<sup>1,2</sup>, J. J. Wu<sup>1,2</sup>, A. C. Wilson<sup>1,2</sup>, D. J. Wineland<sup>1,2,3</sup>, and D. Leibfried<sup>†1,2</sup>

<sup>1</sup>National Institute of Standards and Technology, Time and Frequency Division 688, 325  
Broadway, Boulder, CO 80305, USA

<sup>2</sup>Department of Physics, University of Colorado, Boulder, CO 80305, USA

<sup>3</sup>University of Oregon, Department of Physics, Eugene, OR 97403, USA

## Abstract

A mixed-species geometric phase gate has been proposed for implementing quantum logic spectroscopy on trapped ions, which combines probe and information transfer from the spectroscopy to the logic ion in a single pulse. We experimentally realize this method, show how it can be applied as a technique for identifying transitions in currently intractable atoms or molecules, demonstrate its reduced temperature sensitivity, and observe quantum-enhanced frequency sensitivity when applied to multi-ion chains. Potential applications include improved readout of trapped-ion clocks and simplified error syndrome measurements for quantum error correction.

## 1 Introduction

Quantum logic spectroscopy (QLS) can be used for internal-state preparation and readout for atomic and molecular ion species that lack a suitable electronic level structure to directly implement these tasks [1, 2, 3, 4]. In principle, through the use of a “logic ion” (LI) and its motional coupling to a co-trapped “spectroscopy ion” (SI), QLS allows control over any ion species. The traditional QLS protocol, as presented in [1], has two main limitations. First, it requires the ions to be cooled to near the motional ground state. Second, its readout efficiency scales poorly with the number of SIs, which could pose an obstacle to achieving the improved stability that could come from scaling quantum-logic-enabled atomic clocks to multiple ions [5]. Methods have been developed to mitigate these effects using repetitive quantum nondemolition (QND) measurements [6, 7, 8]. However,

applying them might not be possible due to an unsuitable electronic structure, and repetitive measurements will decrease the duty cycle of the spectroscopy probe.

Here we demonstrate a QLS method proposed in [9] based on a geometric phase gate that is often used in quantum information processing for multi-qubit entangling gates. This type of geometric phase gate has previously been used on a mixed-species ion pair to implement quantum logic readout with reduced temperature sensitivity as part of a controlled-NOT operation [10]. In that experiment, the interrogation and detection of the SI were accomplished with separate laser operations. Here we explore a technique, using only a Mølmer-Sørensen (MS) interaction [11, 12, 13, 14, 15], to simultaneously implement both the spectroscopy operation and transfer of SI state information to the LI for readout. This reduces temperature sensitivity compared to traditional QLS. Additionally, the technique can be applied to multiple SIs, for which it features Heisenberg-limited spectroscopic sensitivity [16, 17]. While our technique shares some features with previous work, which implemented Heisenberg-limited Ramsey [18, 19] and Rabi spectroscopy [20], it extends metrology that takes advantage of entanglement to a wider range and number of spectroscopy ions [9].

## 2 Description of the method

### 2.1 Basic operations

We consider the LI and SI as effective two-level (spin-1/2) systems, with measurement-basis states labeled  $\{|\uparrow_{\text{LI}}\rangle, |\downarrow_{\text{LI}}\rangle\}$  and  $\{|\uparrow_{\text{SI}}\rangle, |\downarrow_{\text{SI}}\rangle\}$  respectively. The LI and SI are coupled through a shared harmonic oscillator normal mode of motion with frequency  $\omega_m$  and eigenstates  $|n\rangle$ . To implement the spectroscopy scheme, we require interactions that can drive motional sideband transitions  $|\downarrow\rangle |n\rangle \leftrightarrow |\uparrow\rangle |n \pm 1\rangle$  on the LI and SI independently with “+” denoting a “blue” sideband (BSB) and “−” a “red”

<sup>\*</sup>Authors D.K. and Y.W. have contributed equally to this work.

<sup>†</sup>Current address: ETH Zurich, Otto-Stern-Weg 1, HPF E10, 8093 Zurich, Switzerland

<sup>‡</sup>Corresponding author, email: dietrich.leibfried@nist.gov

sideband (RSB). Such interactions can be implemented with laser fields [21, 22] and microwave fields [23, 24]. The detuning of the BSB (+) and RSB (−) of the LI relative to the spin transition is given by  $\delta_{\text{LI}} = \pm(\omega_m + \delta_{\text{MS}})$  while for the SI it is  $\delta_{\text{SI}} = \pm(\omega_m + \delta_{\text{MS}}) + \delta_S$ . The detuning  $\delta_{\text{MS}}$  is equal for the LI and SI sidebands and serves to implement the MS interaction [13]. The SI sidebands can be further detuned by a variable  $\delta_S$ , a common detuning of the BSB and RSB that enables scans to locate the SI resonance frequency, which would initially be unknown in a general spectroscopy experiment. Note that  $\omega_m$  and  $\delta_{\text{MS}}$  can be calibrated with experiments on the LIs without prior knowledge of SI properties.

For simplicity, consider  $M$  SIs and  $N$  LIs, where either  $N = 1$  and  $M$  is odd or both  $M$  and  $N$  are even, and all ions have equal sideband Rabi frequencies  $\Omega_{\text{sb}}$ . In both cases, if the BSBs and RSBs are applied simultaneously and on resonance ( $\delta_S = 0$ ) for  $t_{\text{MS}} = 4\pi/\delta_{\text{MS}}$  (twice the duration of a typical MS entangling operation  $U_{\text{MS}}$ ), and with detuning  $\delta_{\text{MS}} = 4\Omega_{\text{sb}}$ , the system undergoes (up to a global phase factor) a complete spin-flip

$$U_{\text{MS}}^2 = \sigma_{\mathbf{x}}^{(1)} \otimes \sigma_{\mathbf{x}}^{(2)} \otimes \dots \otimes \sigma_{\mathbf{x}}^{(M+N)}. \quad (1)$$

Here  $\sigma_j^{(i)}$  are the Pauli operators ( $j \in \{x, y, z\}$ ) acting on ion  $i$ . In contrast, if the SIs are far off resonance ( $\delta_S \gg \Omega_{\text{sb}}$ ), only the  $N$  LIs partake in the MS interaction. We will call this operation a “mutually-controlled multi-flip” (shortened to “multi-flip” in the following). See Appendix A.2 for the full MS Hamiltonian and details of the implementation.

For  $N = 1$  and the SIs far off resonance, the effect on the single LI is just a phase factor  $e^{i\pi/4}$ . Crucially, irrespective of the initial states of SIs and LI, *all* spins flip if the SIs are on resonance, while they *all* remain the same (up to a phase factor) if the SIs are far off resonance. For intermediate detuning,  $\delta_S \simeq \Omega_{\text{sb}}$ , the dynamics are complicated, leading to substantial populations in several basis states. The probability of the LI flipping as a function of  $\delta_S$  (i.e. the spectral line-shape) is not straightforward to express analytically and depends on the temperature of the motional mode, but qualitatively the logic ion continuously transfers from no flip to a full flip as  $\delta_S$  is swept from far detuned to resonance.

For  $M$  and  $N$  even, and with the SIs far off resonance, the LIs undergo the usual MS interaction in their subspace while the SIs are unaffected, described by

$$\mathbf{I}_{\text{SI}} \otimes \sigma_{\mathbf{x}}^{(1)} \otimes \sigma_{\mathbf{x}}^{(2)} \otimes \dots \otimes \sigma_{\mathbf{x}}^{(N)}, \quad (2)$$

where  $\mathbf{I}_{\text{SI}}$  is the identity operator acting on all  $M$  SIs and  $\sigma_x^{(i)}$  acts on LI  $i \in \{1, \dots, N\}$ . With the SIs on resonance or far off resonance, the LIs flip, but other states are populated for an intermediate detuning  $\delta_S \simeq \Omega_{\text{sb}}$  leading to a characteristic, temperature-dependent line-shape. Generalizing to other numbers of SIs and LIs complicates the discussion, but does not change the basic mechanism [25].

In all cases, the multi-flip does not depend on the initial states of the two species and retains the reduced temperature sensitivity of the MS interaction in the Lamb-Dicke (LD) regime [13], so it can be used as a robust combined spectroscopy probe and readout method. As described so far, the multi-flip is analogous to Rabi spectroscopy and ideally achieves a Fourier-limited frequency resolution of  $\sim 1/t_{\text{MS}}$  when scanning the detuning  $\delta_S$ . The characteristics of Ramsey spectroscopy appear when the MS interaction is applied twice with a duration of  $t_{\text{MS}}/2$  (effective  $\pi/2$ -pulses) before and after a period  $T_{\text{R}}$  of free evolution. Analogous to traditional Ramsey spectroscopy, this sequence ideally achieves Fourier-limited frequency resolution ( $1/T_{\text{R}}$  for a single SI) if the effective  $\pi/2$ -pulses are much shorter than the Ramsey free evolution time, i.e.  $t_{\text{MS}} \ll T_{\text{R}}$ . As discussed in the next section, for more SIs driven on resonance,  $M$ -partite entangled “Schrödinger-cat spin states” [26, 27, 19] evolve during  $T_{\text{R}}$  to ideally achieve Heisenberg-limited resolution.

## 2.2 Heisenberg scaling

If the multi-flip is applied to multiple SIs, they transition through an entangled state during the probe (this occurs naturally for the MS interaction on resonance [10]), resulting in increased frequency sensitivity, i.e. providing Heisenberg scaling with the number of SIs [17, 18, 19, 9, 20]. This becomes especially clear in the Ramsey version of the protocol. For example, if an ensemble of  $N$  SIs and  $M$  LIs ( $N, M$  even) is prepared in the spin-up state  $|\uparrow_1, \uparrow_2, \dots, \uparrow_{N+M}\rangle$ , the first Ramsey pulse will result in a “Schrödinger-cat spin state” for the SIs and LIs. Its evolution is then mapped onto the LIs with the second Ramsey pulse. The LIs being part of the entangled state does not add frequency sensitivity. In principle a single LI would suffice, although a larger number of LIs could result in a better detection signal (for example, with three or more LIs one can do a majority vote to decide whether the SIs have flipped or not) and improve the initial cooling of the mixed-species ion chain. For best performance and the simplest implementation, the mode of motion being driven in the MS interaction should ideally have the same mode amplitudes for all ions of the same species. For long ion chains this could be approximately achieved by using the in-phase mode of motion (see Appendix C).

## 2.3 Influence of LI properties on the protocol

We note that by symmetry between the LIs and SIs in this protocol, any detuning of the LIs from resonance will shift the line-center in Rabi spectroscopy and the fringe pattern in Ramsey spectroscopy. In addition, any decoherence of the SIs or LIs will reduce the contrast

of the signal. If the LIs have worse stability or coherence than the SIs (which could be the case in an atomic clock) a frequency shift or loss of contrast due to the LIs can be reduced by dynamically decoupling them. This can be accomplished by dividing the MS interaction into equal-duration sections and interspersing suitable  $\pi$ -pulses that act only on the LIs (see Appendix B for example sequences). Since noise in both the SI and LI lasers perturbs the spectroscopy signal equally, the absolute frequency stability of the LI transition needs to be better than that of the SI transition. This condition could be satisfied if the LI transition frequency is much lower than the SI transition frequency, for example by using an optical transition for the SIs and a hyperfine transition for the LIs. The dependence of the LI's spin population on both the LI and SI can also be used to implement an "atomic combination clock" using two clock species [28], where one of the clock species would not need direct readout.

### 3 Implementation and Results

#### 3.1 Basic method

We demonstrate the basic features of this method on a mixed-species ion pair of electronic ground-state hyperfine qubits composed of one SI ( $^{25}\text{Mg}^+$  with the two-level system defined as  $|\uparrow\rangle_{\text{Mg}} = |3, 1\rangle$  and  $|\downarrow\rangle_{\text{Mg}} = |2, 0\rangle$ , with a frequency splitting  $\omega_{\text{Mg}} \approx 2\pi \times 1.7632$  GHz at the applied magnetic field of  $B \approx 11.9$  mT) and one LI ( $^9\text{Be}^+$  with  $|\uparrow\rangle_{\text{Be}} = |1, 1\rangle$ ,  $|\downarrow\rangle_{\text{Be}} = |2, 0\rangle$ , with a frequency splitting  $\omega_{\text{Be}} \approx 2\pi \times 1.2075$  GHz at the same magnetic field), with the MS interaction implemented on the in-phase mode of motion along the (axial) direction defined by the line connecting the equilibrium positions of both ions. We perform Rabi- and Ramsey-type experiments with both axial modes of motion initially cooled to the ground-state, while the LI is prepared in  $|\uparrow\rangle$  and the SI in either  $|\uparrow\rangle$  or  $|\downarrow\rangle$ . We repeat this procedure for a range of values of  $\delta_{\text{S}}$  and detect both the LI and SI spin states (see Appendix A.1 for details on cooling, state preparation, state detection and the MS interaction). The LI is driven on resonance throughout the entire series of experiments.

As predicted for the multi-flip protocol, both the LI and SI show a clear simultaneous resonance at  $\delta_{\text{S}} = 0$ , independent of the initial SI states (Fig. 1 (a), (b)). The asymmetries visible at larger detuning arise from the red-/blue-detuned light fields of the MS interaction becoming resonant with red or blue sideband transitions when  $\delta_{\text{S}} = \pm\delta_{\text{MS}}$ . For large values of  $\delta_{\text{S}}$ , the spin states of both ions remain unchanged. To fit the full spectrum of these Rabi-type experiments we numerically simulate the evolution of the full system Hamiltonian without making the LD approximation, truncating the harmonic oscillator Hilbert space at  $n = 10$ . We fit the result-

ing spin populations to the data. We use the parameter  $c$  to define  $\Omega_{\text{MS(LI)}} = c\Omega_{\text{MS}}$  and  $\Omega_{\text{MS(SI)}} = \Omega_{\text{MS}}/c$  and optimize by varying  $c$ ,  $\Omega_{\text{MS}}$ ,  $\delta_{\text{MS}}$ , and  $t_{\text{MS}}$ . We chose this parametrization of the Rabi frequencies because  $\Omega_{\text{MS}}^2 = \Omega_{\text{MS(LI)}}\Omega_{\text{MS(SI)}}$  is calibrated precisely, but we cannot assume  $c = 1$  because we do not precisely calibrate the SI and LI Rabi rates separately. We find good agreement between the data and fit. In principle it is possible to set  $c > 1$  deliberately if the SI laser intensity is too low to achieve  $\Omega_{\text{MS(SI)}} = \Omega_{\text{MS(LI)}}$  and increasing the gate duration would lead to detrimental effects. These experiments confirm that the initial spin state of the SI does not significantly impact the spectroscopy signal of the LI and that the LI's signal faithfully represents the SI's spin resonance.

When cooling the ions to the ground state and sweeping  $\delta_{\text{S}}$  in a Ramsey-type experiment with free evolution time  $T_{\text{R}} = 1$  ms, we observe the expected sinusoidal pattern for both species with a contrast in the LI signal of 0.89(1) (Fig. 1 (c)). The imperfect signal contrast, caused by experimental error sources (the leading contributions are most likely relative phase fluctuations between the Raman beam pairs), reduces the frequency sensitivity of the measurement (slope) by a factor equal to the contrast. This is not a fundamental limit of the method and could be improved by reducing the experimental errors.

#### 3.2 Robustness of the method

To demonstrate the robustness of the multi-flip, we perform two sets of experiments under non-ideal conditions. In the first instance we investigate the effects of unwanted residual thermal motion. Instead of ground-state cooling, we only Doppler cool the LI of the ion pair (resulting in thermal states with mean occupations of  $\bar{n} = 3.3(5)/1.7(1)$  for the axial in-phase/out-of-phase modes of motion; the MS interaction is again implemented using the in-phase mode). We tune the Rabi frequencies for both species to the optimal values. The LI shows a resonance with a contrast of  $\approx 65\%$  in a Rabi experiment (Fig. 1 (d)) and 57(2)% in a Ramsey experiment (Fig. 1 (e)). Here, the reduction in contrast can be attributed to the relatively high LD-parameters of our experiment ( $\eta_{\text{Be}} \approx 0.17$  and  $\eta_{\text{Mg}} \approx 0.29$  for the in-phase mode). From simulations we find a contrast of  $\approx 97\%$  for a Rabi-type experiment using the same thermal excitation as in the experiment ( $\bar{n} = 3.3$ ) but LD-parameters of  $\eta = 0.1$  for LI and SI. This ability to operate with imperfect motional ground state preparation in frequency measurement/clock applications can save time otherwise spent on ground-state cooling, improving the duty cycle (thereby reducing the Dick effect [30, 31]).

In another set of experiments, we consider a case where  $\Omega_{\text{MS}}^2$  is not ideal. This is important because generally for a given choice of  $\Omega_{\text{MS(LI)}}$ , the SI laser intensity needed to

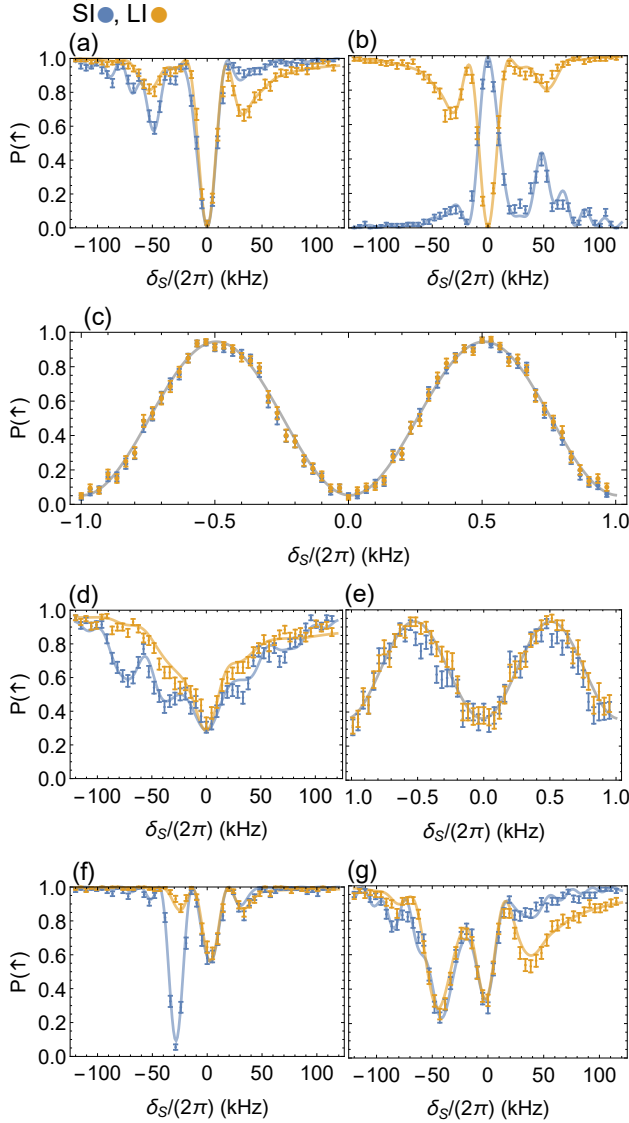


Figure 1: Spin populations for the LI-SI pair (SI: blue, LI: orange). For Rabi experiments (figures a, b, d, f, g) fits are displayed in matching colors. LI populations in Ramsey experiments (c,e) are fit with sinusoids. (a) Rabi spectroscopy with the SI’s spin state initialized to  $|\uparrow_{\text{SI}}\rangle$ , (b) Rabi spectroscopy with the SI’s spin state initialized to  $|\downarrow_{\text{SI}}\rangle$ . (c) Ramsey spectroscopy with a contrast of 0.89(1). (d) Rabi and (e) Ramsey spectroscopy (contrast 0.57(2)) with Doppler cooling only. Rabi spectroscopy with (f)  $\Omega_{\text{SI}} = \Omega_{\text{MS}}/2$  and (g)  $\Omega_{\text{SI}} = 2\Omega_{\text{MS}}$ . In all figures, error bars are calculated assuming quantum projection noise only [29]. Each data point represents the average outcome of 200 repetitions of the experiment (100 for figure e).

provide the corresponding ideal  $\Omega_{\text{MS(SI)}}$  may not initially be known. We ground-state cool the ion pair, and set the Rabi frequency  $\Omega_{\text{MS(SI)}}$  of the SI MS interaction to roughly half (Fig. 1 (f)) or twice the optimal value  $\Omega_{\text{MS}}$

(Fig. 1 (g)). The experiment with the SI Rabi frequency reduced (increased) by a factor of two shows a contrast of  $\approx 40\%$  ( $\approx 70\%$ ) in the LI signal, which is still centered at  $\delta_{\text{S}} = 0$ . In addition to the reduction in contrast, the LI signal exhibits increased side-lobes when the SI is overdriven.

For  $\Omega_{\text{MS(SI)}} = 2\Omega_{\text{MS}}$ , the additional resonances where the blue- (red-)detuned frequency component of the MS interaction is resonant with the blue (red) sideband transition ( $\delta_{\text{S}} = \pm\delta_{\text{m}}$ ) are more strongly pronounced. This implies that one should under-drive the SI once a resonance is found to make the interpretation of the line-shape more straightforward. Counter-intuitively, the SI signal shows a much stronger sideband resonance when it is under-driven (Fig. 1(f)). This is because the weakened MS interaction causes reduced coupling between the spins. When  $\Omega_{\text{SI}} > \Omega_{\text{MS}}$ , the MS interaction increases, causing the LI and SI spectra to overlap over a larger range of detunings.

We fit all datasets as described in section 3.1. When fitting the Doppler-cooled data, the harmonic oscillator Hilbert space is truncated at  $n = 20$  and a thermal state with  $\bar{n} = 3.3$  is used as the initial state.

For comparison, simulations of traditional QLS using the thermal excitation measured in the experiment with just Doppler cooling give a contrast of  $\approx 23\%$  in a Ramsey sequence (compared to  $\approx 57\%$  with the multi-flip). The pulse durations are optimized numerically for best contrast. Both the pulse durations and the contrast depend on the temperature. Lowering the LD-parameter as proposed for the multi-flip when using Doppler cooling results in a decrease of the contrast for the traditional QLS. For the above simulated example of  $\bar{n} = 3.3$  and LD-parameters  $\eta = 0.1$  for both the LI and SI, the traditional QLS would result in a contrast of  $\approx 18\%$ . With the SI Rabi frequency reduced by a factor of two in a Rabi sequence using the traditional QLS we predict a contrast of 50% (compared to  $\approx 40\%$  for the multi-flip). With the SI Rabi frequency increased by a factor of two in the traditional QLS no usable signal exists on resonance, but symmetric side peaks at  $\approx \pm 2\pi \times 300$  kHz relative to the resonant frequency show a contrast of  $\approx 47\%$ , which could also be used to identify the transition (compared to  $\approx 70\%$  on resonance for the multi-flip). We conclude that imperfect Rabi-frequency settings affect both the traditional QLS and multi-flip roughly equally.

### 3.3 Demonstration of Heisenberg scaling

Finally, we demonstrate the behavior of the multi-flip for larger systems of ions and the naturally-arising Heisenberg scaling for frequency sensitivity. We use a four-ion linear chain of two SIs ( $^{25}\text{Mg}^+$ ) and two LIs ( $^9\text{Be}^+$ ). The ions in the chain are ordered  $^9\text{Be}^+ - ^{25}\text{Mg}^+ - ^{25}\text{Mg}^+ - ^9\text{Be}^+$ . We implement the MS interaction on the mo-

tional mode in the axial direction, for which the  ${}^9\text{Be}^+ - {}^{25}\text{Mg}^+$  pair of the chain oscillates out of phase with the remaining  ${}^{25}\text{Mg}^+ - {}^9\text{Be}^+$  pair. All axial motional modes are cooled to the ground state and the spin state of the ions is initialized to  $|\uparrow_{\text{LI}}\uparrow_{\text{SI}}\uparrow_{\text{SI}}\uparrow_{\text{LI}}\rangle$ . We perform a Ramsey-type experiment (Fig. 2) with free evolution time  $T_{\text{R}} = 500 \mu\text{s}$  and observe a contrast of 75(2)% with the same Ramsey fringe oscillation frequency as the two-ion experiment for  $T_{\text{R}} = 1 \text{ ms}$ , consistent with Heisenberg scaling.

### 3.4 Applications in quantum information processing

The multi-flip can be used on resonance ( $\delta_{\text{S}} = 0$ ) as a QND measurement method to detect if the SI (or qubit) is in the intended two-level manifold. In particular, if the SI can be described as a three-level system, with levels  $a$  and  $b$  defining a qubit and  $c$  an auxiliary state, the multi-flip can be used to detect any leakage into level  $c$ , which in a quantum information processing context would be described as a *leakage error*. When the multi-flip is applied to the  $a$ - $b$  state-manifold, the final state of the LI will indicate if a leakage event has occurred and if not, the qubit can be restored with a single-qubit rotation that reverses the rotation of the SI caused by the multi-flip. Leakage will be relevant at some level for almost any quantum information or spectroscopy application.

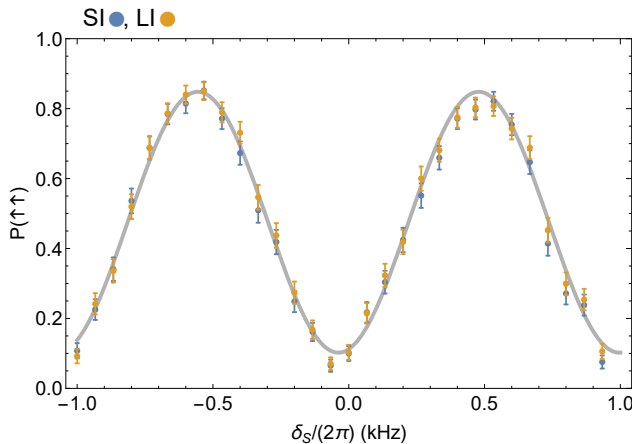


Figure 2: Spin populations for the four-ion chain LI-SI-SI-LI (SI: blue, LI: orange), initially prepared in the spin state  $|\uparrow_{\text{LI}}\uparrow_{\text{SI}}\uparrow_{\text{SI}}\uparrow_{\text{LI}}\rangle$ , performing Ramsey spectroscopy with free evolution time  $T_{\text{R}} = 500 \mu\text{s}$ . The data shows the same Ramsey-fringe oscillation frequency as the LI-SI data with  $T_{\text{R}} = 1 \text{ ms}$ , consistent with Heisenberg scaling. We fit a sinusoidal curve (solid curve) to the LI-LI data and extract a contrast of 75(2)%. In this experiment  $t_{\text{MS}} \approx 64 \mu\text{s}$ . Error bars are calculated assuming quantum projection noise only. Each data point represents the average outcome of 200 repetitions of the experiment.

Streamlined QND detection of this error could reduce error-correction overhead [32]. Similar ideas about the use of the multi-flip for detecting leakage errors were contemplated by Schindler et al. [33].

The multi-flip could also be used as a general QND readout method of the populations of a two-level system in trapped ions: invoking the three-level model described in the previous paragraph, the MS multi-flip could be used to determine the populations of the states  $a$  and  $b$  by applying the multi-flip to the state manifolds  $a$ - $c$  or  $b$ - $c$ . This QND measurement could also be used to improve readout fidelity in frequency measurement and clock applications with potentially fewer repeated applications compared to [6, 7, 8] due to higher single-shot fidelity.

## 4 Conclusion

We have demonstrated a new method for QLS based on the MS interaction using a mixed-species ion system, showing its basic behavior, its robustness to experimental imperfections and how it scales to larger systems. This “multi-flip” technique provides a spectroscopy method with improved readout performance compared to traditional QLS. Additionally, it can be used as a combined multi-ion-clock probe and readout technique, naturally providing Heisenberg scaling, which could help improve the stability of ion-based optical clocks. Further applications of the multi-flip in quantum information include optimized QND error-syndrome measurements, which may help to scale future trapped-ion quantum computers to larger numbers of qubits. The MS multi-flip could also be generalized to other systems where oscillators can be coupled to two-level systems, such as superconducting circuits, the ro-vibrational levels of a molecule or micro/nanomechanical resonators.

**Acknowledgments** The authors thank S. C. Burd and D. B. Hume for helpful comments on the manuscript. D.K., Y.W., and J.J.W. acknowledge support of the Professional Research Experience Program (PREP) operated jointly by NIST and University of Colorado Boulder. This work was supported by the Office of the Director of National Intelligence (ODNI) Intelligence Advanced Research Projects Activity (IARPA), and the NIST Quantum Information Program. D.K. acknowledges support from the Swiss National Science Foundation under grant no. 165208. S.D.E. acknowledges support by the U.S. National Science Foundation under Grant No. DGE 1650115. This manuscript is a contribution of NIST and not subject to U.S. copyright.

# A Methods

## A.1 State preparation and readout

At the start of each experiment, the  ${}^9\text{Be}^+$  ion (LI) is optically pumped to  $|2, 2\rangle$  in the  $S_{1/2}$  electronic ground state. Similarly, we optically pump the  ${}^{25}\text{Mg}^+$  ion (SI) to the  $|3, 3\rangle$  electronic ground state. This is followed by Doppler cooling of  ${}^{25}\text{Mg}^+$  and then  ${}^9\text{Be}^+$ , implemented by driving the  $S_{1/2} |3, 3\rangle \leftrightarrow P_{3/2} |4, 4\rangle$  cycling-transition for  ${}^{25}\text{Mg}^+$  and the  $S_{1/2} |2, 2\rangle \leftrightarrow P_{3/2} |3, 3\rangle$  cycling transition for  ${}^9\text{Be}^+$  with  $\sigma^+$ -polarized light. For ground-state initialization of both axial modes of the  ${}^9\text{Be}^+$ - ${}^{25}\text{Mg}^+$  ion pair, Raman sideband cooling is applied to the  ${}^9\text{Be}^+$  ion after Doppler cooling [34]. To transfer  ${}^9\text{Be}^+$  to the  $|1, 1\rangle = |\uparrow\rangle_{\text{Be}}$  state we use a microwave composite pulse sequence that is robust against transition-frequency detuning and Rabi frequency errors. The sequence is composed of the following resonant pulses:  $R(\pi, 0)$ ,  $R(\pi, 5\pi/6)$ ,  $R(\pi, \pi/3)$ ,  $R(\pi, 5\pi/6)$ ,  $R(\pi, 0)$  [35], where  $R(\theta, \phi)$  is the single-spin rotation defined as

$$R(\theta, \phi) = \begin{pmatrix} \cos(\theta/2) & -ie^{-i\phi} \sin(\theta/2) \\ -ie^{i\phi} \sin(\theta/2) & \cos(\theta/2) \end{pmatrix}. \quad (3)$$

With analogous pulse sequences, the  ${}^{25}\text{Mg}^+ |3, 3\rangle$  state is transferred to the  $|2, 2\rangle$  state and subsequently to the  $|3, 1\rangle = |\uparrow\rangle_{\text{Mg}}$  state.

To measure the qubit states the initial mapping procedure is reversed, putting the  $|\uparrow\rangle_{\text{Be}}$ ,  $|\uparrow\rangle_{\text{Mg}}$  states back in their respective cycling transition ground states. The  $|\downarrow\rangle_{\text{Be}} \equiv |2, 0\rangle$ ,  $|\downarrow\rangle_{\text{Mg}} \equiv |2, 0\rangle$  states are shelved to  $|1, -1\rangle$  and  $|2, -2\rangle$ , respectively, using a single microwave  $\pi$ -pulse for the  ${}^9\text{Be}^+ |2, 0\rangle \rightarrow |1, -1\rangle$  transition and composite pulse sequences for the  $|2, 0\rangle \rightarrow |3, -1\rangle$  and  $|3, -1\rangle \rightarrow |2, -2\rangle$  transitions of  ${}^{25}\text{Mg}^+$ . We subsequently apply the Doppler-cooling laser beams tuned to resonance and collect the fluorescence light of the ions with an achromatic imaging system designed for both 313 nm and 280 nm light [36]. With a detection duration of 330  $\mu\text{s}$  for  ${}^9\text{Be}^+$  (200  $\mu\text{s}$  for  ${}^{25}\text{Mg}^+$ ), we detect on average 30 photons per ion when they are in the  $|2, 2\rangle$  ( $|3, 3\rangle$ ) state and 1.9 (0.7) photons when they are in the  $|1, -1\rangle$  ( $|2, -2\rangle$ ) state (predominantly from light scattered by the trap structure). The qubit state is determined by choosing a photon-count threshold of 10 counts such that the states are maximally distinguished. To prepare the initial state of the four-ion string  ${}^9\text{Be}^+ {}^{25}\text{Mg}^+ {}^{25}\text{Mg}^+ {}^9\text{Be}^+$  we use the same techniques and ground-state cool all four axial modes. Here the qubit states are determined by fitting Poissonian distributions to histograms of the count data.

## A.2 Mølmer-Sørensen interaction, four-ion entangled state

The MS Hamiltonian in the interaction picture can be written (neglecting fast rotating terms, in the LD regime,

and for a single motional mode) as

$$\hat{H} = \hbar \sum_j \Omega_{\text{MS},j} (\hat{\sigma}_j^+ \hat{a} e^{-i((\delta_{\text{S},j}-\delta_{\text{m}})t)+\phi_r} + \hat{\sigma}_j^- \hat{a}^\dagger e^{-i((\delta_{\text{S},j}+\delta_{\text{m}})t)+\phi_b}) + H.c., \quad (4)$$

where the sum runs over the number of ions with  $j$  labeling the ion and  $\Omega_{\text{MS},j}$  the Rabi frequency for each ion, defined as  $\Omega_{\text{MS},j} = \eta_j \Omega_{0,\text{MS},j}$  with  $\Omega_{0,\text{MS},j}$  the bare Rabi frequency of each ion and  $\eta_j = \delta k_j z_{0,j} b_j$  the respective ion's LD parameter. The difference of the  $k$ -vectors of the Raman beams addressing the  $j$ th ion is given by  $\delta k_j$ ,  $b_j$  is the normalized motional mode amplitude of the  $j$ th ion, and  $z_{0,j} = \sqrt{\hbar/(2m_j\omega_m)}$  with  $m_j$  is the mass of the  $j$ th ion and  $\omega_m$  the oscillation frequency of the motional mode used. The detuning from the motional mode is  $\delta_m$ ,  $t$  the duration,  $\delta_{\text{S},j}$  the detuning from the respective ion's spin transition,  $\hat{\sigma}_j^+$  the respective ion's spin raising operator, and  $\hat{a}$  ( $\hat{a}^\dagger$ ) the lowering (raising) operator of the motional mode used. Without loss of generality, we can set all optical phases to zero. Unless otherwise noted the Rabi frequencies are assumed to be equal for all ions ( $\Omega_{\text{MS},j} = \Omega_{\text{MS}}$ ). The implementation of the MS interaction on the two-ion pair is as described in [10] with the difference that the MS interaction is implemented on the axial in-phase mode of motion which has an oscillation frequency of  $\approx 2\pi \times 2.1$  MHz, resulting in LD parameters of  $\eta_{\text{Be}} \approx 0.17$  and  $\eta_{\text{Mg}} \approx 0.29$  for the two species. We choose to implement the MS interaction for the four-ion chain (ordered  ${}^9\text{Be}^+ {}^{25}\text{Mg}^+ {}^{25}\text{Mg}^+ {}^9\text{Be}^+$ ) on the motional mode in the axial direction, for which the  ${}^9\text{Be}^+ {}^{25}\text{Mg}^+$  part of the chain oscillates out of phase with the remaining  ${}^{25}\text{Mg}^+ {}^9\text{Be}^+$  part, which has an oscillation frequency of  $\approx 2\pi \times 3.1$  MHz, resulting in LD parameters of  $|\eta_{\text{Be}}| \approx 0.17$  and  $|\eta_{\text{Mg}}| \approx 0.14$  for the two species. When applying the MS interaction to the state  $|\uparrow_{\text{Be}} \uparrow_{\text{Mg}} \uparrow_{\text{Mg}} \uparrow_{\text{Be}}\rangle$  for a duration  $t = 2\pi/\delta_{\text{MS}} \approx 66 \mu\text{s}$  we measure a state fidelity of 0.937(6) for the four-ion Schrödinger-cat type state  $(|\uparrow_{\text{Be}} \uparrow_{\text{Mg}} \uparrow_{\text{Mg}} \uparrow_{\text{Be}}\rangle + i |\downarrow_{\text{Be}} \downarrow_{\text{Mg}} \downarrow_{\text{Mg}} \downarrow_{\text{Be}}\rangle) / \sqrt{2}$ , by performing an analysis of spin populations and spin parity measurements [37]. For this we measure the spin state of each ion individually by splitting the  ${}^9\text{Be}^+ {}^{25}\text{Mg}^+ {}^{25}\text{Mg}^+ {}^9\text{Be}^+$  ion chain into two  ${}^9\text{Be}^+ {}^{25}\text{Mg}^+$  ion pairs and detecting them sequentially by shuttling the pairs individually into the region where the detection laser beams are focused.

## B Example for dynamical decoupling of the LI

Simple pulse sequences for dynamical decoupling of the LI with  $\pi$ -pulses is given by the following. For Rabi-type spectroscopy:  $U_{\text{MS}}(t_{\text{MS}}/4)$ ,  $R_{\text{LI}}(\pi, 0)$ ,  $U_{\text{MS}}(t_{\text{MS}}/4)$ ,  $R_{\text{LI}}(\pi, 0)$ ,  $U_{\text{MS}}(t_{\text{MS}}/4)$ ,  $R_{\text{LI}}(\pi, 0)$ ,  $U_{\text{MS}}(t_{\text{MS}}/4)$ , where

$U_{\text{MS}}(t)$  is the MS interaction applied for a duration  $t$  and  $R_{\text{LI}}(\theta, \phi)$  is a rotation of the LI spin as defined in Appendix A.1. For Ramsey-type spectroscopy:  $U_{\text{MS}}(t_{\text{MS}}/4)$ ,  $R_{\text{LI}}(\pi, 0)$ ,  $U_{\text{MS}}(t_{\text{MS}}/4)$ ,  $U_{\text{free}}(T_{\text{R}}/2)$ ,  $R_{\text{LI}}(\pi, 0)$ ,  $U_{\text{free}}(T_{\text{R}}/2)$ ,  $U_{\text{MS}}(t_{\text{MS}}/4)$ ,  $R_{\text{LI}}(\pi, 0)$ ,  $U_{\text{MS}}(t_{\text{MS}}/4)$ , where  $U_{\text{free}}(t)$  is the free evolution for the duration  $t$ . Using simulations, we find that a sequence with only a single  $\pi$ -pulse after half the Rabi or Ramsey sequence mirrors the detuned resonance feature, i.e. the resonance is centered on  $-\delta_{\text{S(LI)}}$  instead of  $\delta_{\text{S(LI)}}$  when the MS interaction is detuned by  $\delta_{\text{S(LI)}}$ .

## C Motional mode amplitudes for long ion chains

For high multi-flip contrast, the Rabi frequencies of all LIs and SIs should be the same. This can be challenging in long ion chains because the mode amplitudes will in general be different for ions along the chain. However, this effect is least pronounced for the axial in-phase mode of motion. To demonstrate this, we calculate the mode amplitudes for  $^{40}\text{Ca}^+$ ,  $^{27}\text{Al}^+$  chains with different numbers of ions and find that the axial in-phase mode amplitudes for ions of the same species differ by an experimentally insignificant amount. For example, in a symmetric ion chain with 7  $^{27}\text{Al}^+$  and 6  $^{40}\text{Ca}^+$  (alternating) ions confined by a potential with normal mode frequencies for a single  $^{27}\text{Al}^+$  ion of  $2\pi \times \{6, 6.1, 1\}$  MHz (with the lowest value corresponding to the axial direction) we find relative differences in the axial in-phase mode amplitudes for each ion species to be below 1%.

## References

- [1] P. O. Schmidt, T. Rosenband, C. Langer, W. M. Itano, J. C. Bergquist, and D. J. Wineland, “Spectroscopy using quantum logic,” *Science*, vol. 309, pp. 749–752, 2005.
- [2] T. Rosenband *et al.*, “Observation of the  $^1\text{S}_0 \rightarrow ^3\text{P}_0$  clock transition in  $^{27}\text{Al}^+$ ,” *Phys. Rev. Lett.*, vol. 98, p. 220801, 2007.
- [3] F. Wolf, Y. Wan, J. C. Heip, F. Gebert, C. Shi, and P. O. Schmidt, “Non-destructive state detection for quantum logic spectroscopy of molecular ions,” *Nature*, vol. 530, no. 7591, pp. 457–460, 2016.
- [4] C.-W. Chou, C. Kurz, D. B. Hume, P. N. Plessow, D. R. Leibbrandt, and D. Leibfried, “Preparation and coherent manipulation of pure quantum states of a single molecular ion,” *Nature*, vol. 545, pp. 203–207, 05 2017.
- [5] M. Schulte, N. Lörch, I. D. Leroux, P. O. Schmidt, and K. Hammerer, “Quantum algorithmic readout in multi-ion clocks,” *Phys. Rev. Lett.*, vol. 116, p. 013002, Jan 2016.
- [6] J. C. J. Koelemeij, B. Roth, and S. Schiller, “Black-body thermometry with cold molecular ions and application to ion-based frequency standards,” *Phys. Rev. A*, vol. 76, p. 023413, Aug 2007.
- [7] D. B. Hume, T. Rosenband, and D. J. Wineland, “High-fidelity adaptive qubit detection through repetitive quantum nondemolition measurements,” *Phys. Rev. Lett.*, vol. 99, p. 120502, 2007.
- [8] D. B. Hume, C. W. Chou, D. R. Leibbrandt, M. J. Thorpe, D. J. Wineland, and T. Rosenband, “Trapped-ion state detection through coherent motion,” *Phys. Rev. Lett.*, vol. 107, p. 243902, 2011.
- [9] D. Leibfried, “Playing tricks to ions,” *Applied Physics B*, vol. 123, p. 10, Dec 2016.
- [10] T. R. Tan, J. P. Gaebler, Y. Lin, Y. Wan, R. Bowler, D. Leibfried, and D. J. Wineland, “Multi-element logic gates for trapped-ion qubits,” *Nature*, vol. 528, pp. 380–383, 12 2015.
- [11] A. Sørensen and K. Mølmer, “Quantum computation with ions in thermal motion,” *Phys. Rev. Lett.*, vol. 82, pp. 1971–1974, 1999.
- [12] E. Solano, R. L. de Matos Filho, and N. Zagury, “Deterministic bell states and measurement of the motional state of two trapped ions,” *Phys. Rev. A*, vol. 59, pp. R2539–R2543, Apr 1999.
- [13] A. Sørensen and K. Mølmer, “Entanglement and quantum computation with ions in thermal motion,” *Phys. Rev. A*, vol. 62, p. 022311, 2000.
- [14] G. J. Milburn, S. Schneider, and D. F. James, “Ion trap quantum computing with warm ions,” *Fortschr. Physik*, vol. 48, pp. 801–810, 2000.
- [15] D. Leibfried *et al.*, “Experimental demonstration of a robust and high-fidelity geometric two ion-qubit phase gate,” *Nature*, vol. 422, pp. 412–415, 2003.
- [16] S. L. Braunstein, “Quantum limits on precision measurements of phase,” *Phys. Rev. Lett.*, vol. 69, pp. 3598–3601, Dec 1992.
- [17] J. J. Bollinger, W. M. Itano, D. J. Wineland, and D. J. Heinzen, “Optimal frequency measurements with maximally correlated states,” *Phys. Rev. A*, vol. 54, pp. R4649–R4652, Dec 1996.
- [18] D. Leibfried, M. D. Barrett, T. Schaetz, J. Britton, J. Chiaverini, W. M. Itano, J. D. Jost, C. Langer, and D. J. Wineland, “Toward Heisenberg-limited spectroscopy with multiparticle entangled states,” *Science*, vol. 304, pp. 1476–1478, 2004.

- [19] T. Monz, P. Schindler, J. T. Barreiro, M. Chwalla, D. Nigg, W. A. Coish, M. Harlander, W. Hänsel, M. Hennrich, and R. Blatt, “14-qubit entanglement: Creation and coherence,” *Phys. Rev. Lett.*, vol. 106, p. 130506, Mar 2011.
- [20] R. Shaniv, T. Manovitz, Y. Shapira, N. Akerman, and R. Ozeri, “Toward Heisenberg-limited Rabi spectroscopy,” *Phys. Rev. Lett.*, vol. 120, p. 243603, Jun 2018.
- [21] D. J. Wineland, C. Monroe, W. M. Itano, D. Leibfried, B. E. King, and D. M. Meekhof, “Experimental issues in coherent quantum-state manipulation of trapped atomic ions,” *J. Res. Natl. Inst. Stand. Technol.*, vol. 103, pp. 259–328, 1998.
- [22] R. Blatt and D. J. Wineland, “Entangled states of trapped atomic ions,” *Nature*, vol. 453, pp. 1008–1015, 2008.
- [23] M. Johanning, A. Braun, N. Timoney, V. Elman, W. Neuhauser, and C. Wunderlich, “Individual addressing of trapped ions and coupling of motional and spin states using rf radiation,” *Phys. Rev. Lett.*, vol. 102, p. 073004, Feb 2009.
- [24] C. Ospelkaus, U. Warring, Y. Colombe, K. R. Brown, J. M. Amini, D. Leibfried, and D. J. Wineland, “Microwave quantum logic gates for trapped ions,” *Nature*, vol. 476, pp. 181–184, 2011.
- [25] D. Leibfried and D. J. Wineland, “Efficient eigenvalue determination for arbitrary pauli products based on generalized spin-spin interactions,” *Journal of Modern Optics*, vol. 65, no. 5-6, pp. 774–779, 2018.
- [26] C. A. Sackett, D. Kielpinski, B. E. King, C. Langer, V. Meyer, C. J. Myatt, M. Rowe, Q. A. Turchette, W. M. Itano, D. J. Wineland, and C. Monroe, “Experimental entanglement of four particles,” *Nature*, vol. 404, p. 256, 2000.
- [27] D. Leibfried, E. Knill, S. Seidelin, J. Britton, R. B. Blakestad, J. Chiaverini, D. B. Hume, W. M. Itano, J. D. Jost, C. Langer, R. Ozeri, R. Reichle, and D. J. Wineland, “Creation of a six-atom Schroedinger cat state,” *Nature*, vol. 438, pp. 639–642, 2005.
- [28] N. Akerman and R. Ozeri, “Atomic combination clocks,” *ArXiv e-prints*, 09 2017.
- [29] W. M. Itano, J. C. Bergquist, J. J. Bollinger, J. M. Gilligan, D. J. Heinzen, F. L. Moore, M. G. Raizen, and D. J. Wineland, “Quantum projection noise: Population fluctuations in two-level systems,” *Phys. Rev. A*, vol. 47, pp. 3554–3570, May 1993.
- [30] G. J. Dick, “Local oscillator induced instabilities in trapped ion frequency standards,” in *Proc. Precise Time and Time Interval Meeting*, (USNO, Washington), pp. 133–147, 1987.
- [31] G. Santarelli, C. Audoin, A. Makdissi, P. Laurent, G. J. Dick, and A. Clairon, “Frequency stability degradation of an oscillator slaved to a periodically interrogated atomic resonator,” *IEEE Transactions on Ultrasonics, Ferroelectrics, and Frequency Control*, vol. 45, pp. 887–894, July 1998.
- [32] N. C. Brown and K. R. Brown, “Comparing Zeeman qubits to hyperfine qubits in the context of the surface code:  $^{174}\text{Yb}^+$  and  $^{171}\text{Yb}^+$ ,” *Phys. Rev. A*, vol. 97, p. 052301, May 2018.
- [33] P. Schindler, M. Müller, D. Nigg, J. T. Barreiro, E. A. Martinez, M. Hennrich, T. Monz, S. Diehl, P. Zoller, and R. Blatt, “Quantum simulation of dynamical maps with trapped ions,” *Nature Physics*, vol. 9, pp. 361–367, 2013.
- [34] C. Monroe, D. M. Meekhof, B. E. King, S. R. Jefferts, W. M. Itano, D. J. Wineland, and P. Gould, “Resolved-sideband Raman cooling of a bound atom to the 3D zero-point energy,” *Phys. Rev. Lett.*, vol. 75, no. 22, p. 4011, 1995.
- [35] M. H. Levitt, “Composite pulses,” *Progress in Nuclear Magnetic Resonance Spectroscopy*, vol. 18, no. 2, pp. 61 – 122, 1986.
- [36] P. Huang and D. Leibfried, “Achromatic catadioptric microscope objective in deep ultraviolet with long working distance,” 2004.
- [37] C. A. Sackett *et al.*, “Experimental entanglement of four particles,” *Nature*, vol. 404, p. 256, 2000.